RNA (1998), *4*:1179–1185. Cambridge University Press. Printed in the USA.

REPORT

A quantitative study of the flexibility contributed to RNA structures by nicks and single-stranded gaps

SCOTT B. COHEN AND THOMAS R. CECH

Howard Hughes Medical Institute, Department of Chemistry and Biochemistry, University of Colorado, Boulder, Colorado 80309-0215, USA

ABSTRACT

Disulfide crosslinking via thiol–disulfide interchange was applied to quantitate the relative flexibility contributed by nicks and single-stranded gaps in an RNA structure. An RNA duplex comprised of three strands was constructed containing the disulfide crosslink precursors 1 and 2 at opposite ends of the duplex on opposite strands. The third strand was of varying length to yield a nick or single-stranded gaps of 1, 2, or 3 nt. Crosslinking rates indicated relative flexibilities of the resulting two-helix junctions. Crosslinking in the nicked duplex occurred two orders of magnitude slower than in a duplex containing a 3-nt gap. Rates of crosslinking in duplexes with 3-and 2-nt gaps showed only modest dependence on the gap sequence. Many natural RNAs, including ribozymes, contain two-helix junctions related to the model system described here. The data suggest that two-helix junctions containing a nick in one strand will retain substantial rigidity, whereas one or more single-stranded nucleotides at a two-helix junction allow significant flexibility.

Keywords: 2′-amine; crosslinking; disulfide; flexibility; thermal motion; two-helix junction

INTRODUCTION

The abundance of secondary structural features such as single-stranded gaps and bulges within large RNAs allows the formation of compact tertiary structure (Cate et al., 1996; Lehnert et al., 1996). The contribution of such structural features to the conformational dynamics (thermal motions) of large folded RNAs has not been examined systematically.

The development of reagents and methods for attaching crosslinkable groups to the 2′-position of the RNA backbone (Verheyden et al., 1971; Benseler et al., 1992; Sigurdsson et al., 1995) provides new tools for assessing conformational dynamics. As a result, RNA thermal motions could be studied within a 310-nt ribozyme derived from the self-splicing group I intron of *Tetrahymena* using disulfide crosslinking via thiol–disulfide interchange (Scheme 1) (Cohen & Cech, 1997). The distance dependence of disulfide crosslinks revealed the occurrence of thermal motions of at least 50 Å between helical domains. In contrast, when crosslinking precursors **1** and **2** were incorporated on opposite faces of a short, continuous RNA helix, crosslinking was not observed. These results suggested that the surprising amount of flexibility observed within the ribozyme was due to the various single-stranded regions between the base paired regions within the secondary structure. Experiments in this work apply the thiol–disulfide interchange chemistry to a quantitative evaluation of the relative flexibility contributed by nicks and single-stranded gaps of varying length, and its dependence on the sequence of such structural features.

Reprint requests to: Thomas R. Cech, Howard Hughes Medical Institute, Department of Chemistry and Biochemistry, University of Colorado, Boulder, Colorado 80309-0215, USA; e-mail: thomas.cech@colorado.edu.

Application of thiol–disulfide interchange to a three-stranded RNA duplex

The experimental system consists of an RNA duplex comprised of three strands (Fig. 1). The thiol **2** is placed on a 30-mer (blue) and the disulfide **1** is placed on a 13-mer complement (red). The third strand (green), complementary to the remaining portion of the 30-mer, is of varying length such that a 14-mer affords a 3-nt single-stranded gap within the duplex, a 15-mer affords a 2-nt gap, a 16-mer affords a 1-nt gap, and a 17-mer yields a nick lacking only the phosphate. The relative flexibility contributed by the structural features will be inferred

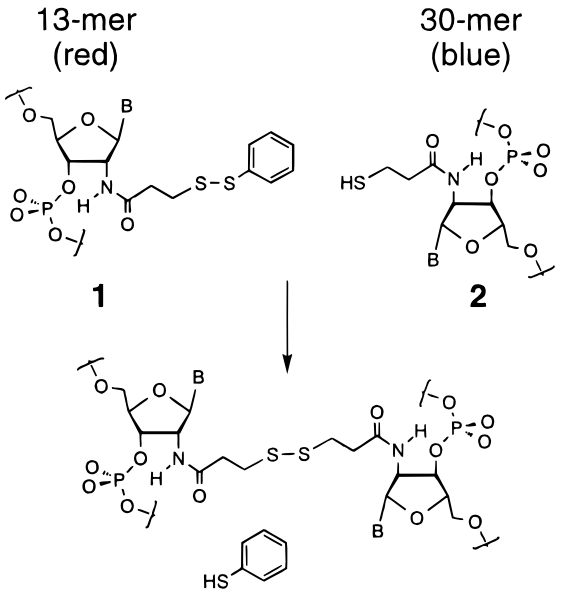

SCHEME 1.

by the rate of crosslinking (Scheme 1) as the disulfide **1** and the thiol **2** become proximal to each other. The RNAs were prepared by solid-phase RNA synthesis with the incorporation of a 2′-amino-2′-deoxy-cytidine at the position of modification (Sigurdsson et al., 1995). The 2′-amine was then modified as described previously (Scheme 2, see Materials and Methods) (Cohen & Cech, 1997).

The crosslinking reactions were conducted with a saturating excess (200 nM) of the thiol-modified 30-mer over a limiting amount of ^{32}P-labeled 13-mer to discourage spurious crosslinking as a result of unassociated disulfide **1**. The third, unmodified strand was present at 300 nM. Annealing of the three-stranded duplex was performed at pH 4.5, where nucleophilic attack by thiol is slow in this system, and completeness of annealing was confirmed by native gel electrophoresis (Fig. 2). Crosslinking was initiated at 50 °C by addition of Tris buffer to attain a final pH of 7.5. The measured (1,500 nM) and corrected (200 nM) UV thermal melting temperatures were 20 °C higher than the working temperature of 50 °C (data not shown), as anticipated from the thermodynamic parameters developed by Turner and co-workers (Freier et al., 1986a). Thus, the duplexes were stable under the crosslinking conditions. Limited experiments at 37 °C found that crosslinking proceeded uniformly slower than at 50 °C; crosslinking was observed clearly in the nicked duplex (data not shown). Experiments were pursued at 50 °C to shorten time courses, thereby obtaining a greater dynamic range in crosslinking rates. Crosslinking typically proceeded to ~50% yield; the reduced yield can be attributed to the less than quantitative modification of the 2′-amines and the oxidation of the thiol during annealing at elevated temperature.

The crosslinking reaction, formally a bimolecular reaction, was independent of strand concentration (Fig. 3), supporting the intrahelical pathway. To test

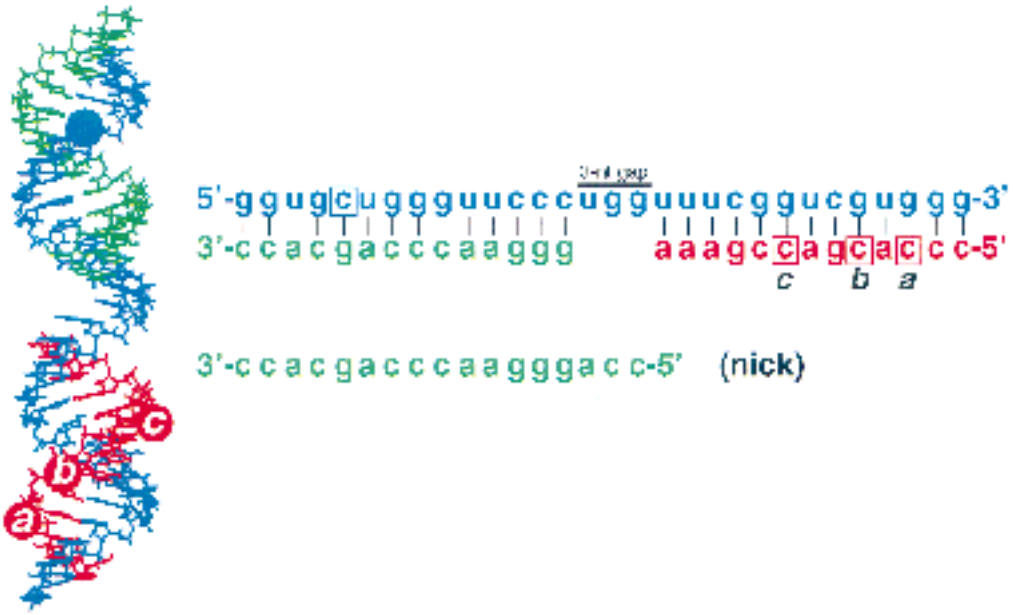

FIGURE 1. Sequence of RNAs in the three-stranded duplex. Model on left drawn with the 14-mer unmodified RNA (green) yielding a 3-nt gap. Spheres represent positions of 2′-thiol (blue) and 2′-disulfide (red) modifications, corresponding to boxed nucleotides in the sequence. ***a***, ***b***, and ***c*** represent three separate 13-mers, each with a single 2′-disulfide at the position indicated.

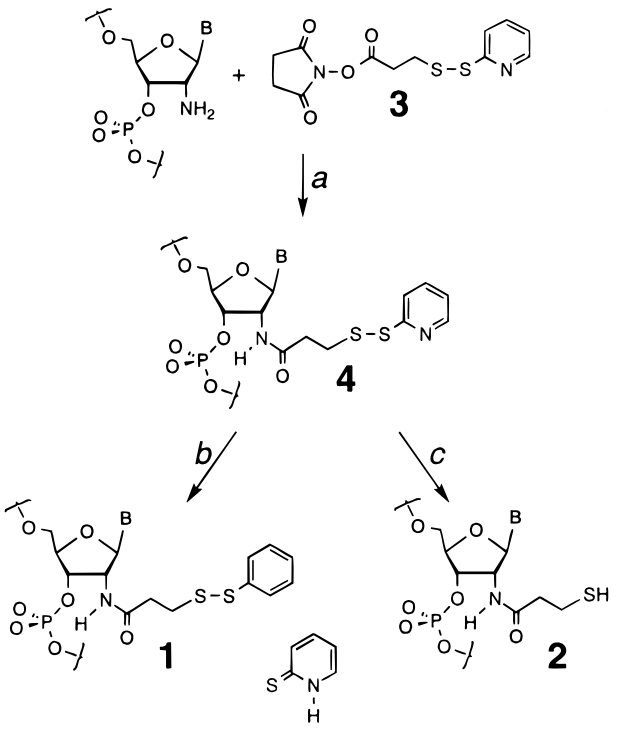

SCHEME 2. Preparation of crosslink precursors **1** and **2**. Reaction conditions as follows. ***a***: RNA with site-specific 2′-amino-2′-deoxyribose substitution (100 μM), aqueous $NaB(OH)_3$ (100 mM, pH 8), NaCl (100 mM), **3** (50 mM), DMF (10% v/v), 37 °C, 30 min. ***b***: C_6H_5-SH (70 mM), 1/1 (v/v) aqueous $NaB(OH)_3$ (100 mM, pH 8)/ethanol, 23 °C, 1 min. ***c***: Dithiothreitol (100 mM), aqueous $NaB(OH)_3$ (100 mM, pH 8), 37 °C, 30 min.

further for the occurrence of any interhelical crosslink-ing, the disulfide **1** and the thiol **2** were annealed on separate duplexes, then mixed to give a final RNA concentration of 200 nM. Interhelical crosslinking was

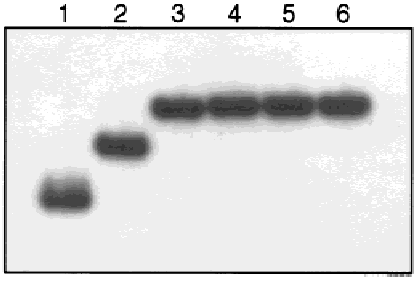

FIGURE 2. Annealing of three-stranded duplex followed by native gel electrophoresis. Annealing was performed with free 2′-amines on 30-mer and 13-mer RNAs (prior to treatment with **3**). Annealing was conducted in HEPES buffer (100 mM, pH 7.5) and sodium chloride (50 mM). Solutions were incubated at 70 °C for 1 min followed by 3 min at 50 °C and electrophoresed in a 15% native polyacrylamide gel at 20 °C (20 W) in HEPES buffer (100 mM, pH 7.5). Lane 1, ^{32}P-labeled 30-mer (5 nM); lane 2, ^{32}P-labeled 30-mer, 13-mer (200 nM); lane 3, ^{32}P-labeled 30-mer, 13-mer (200 nM), unmodified 14-mer (300 nM); lane 4, ^{32}P-labeled 30-mer, 13-mer (200 nM), unmodified 15-mer (300 nM); lane 5, ^{32}P-labeled 30-mer, 13-mer (200 nM), unmodified 16-mer (300 nM); lane 6, ^{32}P-labeled 30-mer, 13-mer (200 nM), unmodified 17-mer (300 nM).

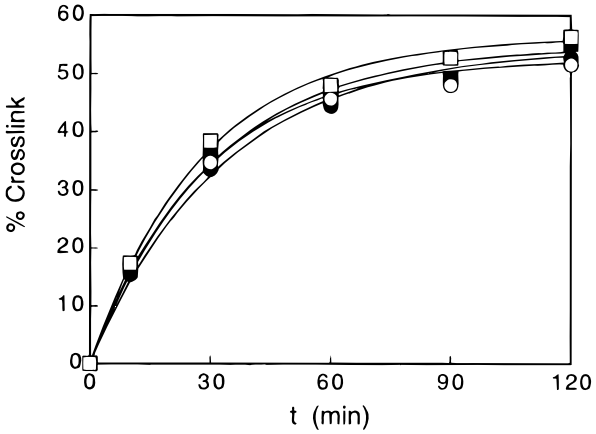

FIGURE 3. Crosslinking as a function of strand concentration in duplex with 2-nt gap. All reactions contained disulfide-modified 13-mer (5 nM, modified at position ***b***), sodium chloride (1 M), sodium acetate (50 mM), disodium EDTA (1 mM), Tris buffer (100 mM, pH 7.5, 50 °C), and varying concentrations of thiol-modified 30-mer and unmodified 15-mer: (●) 100 nM 30-mer, 150 nM 15-mer; (■) 200 nM 30-mer, 300 nM 15-mer; (□) 500 nM 30-mer, 750 nM 15-mer; (○) 1000 nM 30-mer, 1500 nM 15-mer.

not observed over a 6-h period at pH 7.5 (data not shown).

Disulfide crosslinking as an indicator of duplex flexibility

Initial experiments investigated the relative flexibility of various structural features within a constant sequence. Five different crosslinking reactions were performed in parallel; four contained an unmodified strand (Fig. 1, green), yielding duplexes with a nick, 1-, 2-, or 3-nt gap; the fifth reaction lacked the unmodified strand, yielding a 17-nt single-stranded overhang. With the disulfide at position ***b***, five base pairs from the 5′ end (Fig. 1), significant variation in the time course of crosslinking was observed, spanning minutes to several hours (Fig. 4; Table 1, column ***b***). Each rate profile could be fit with a single rate constant, indicative of a homogeneous population of RNA molecules. There was a step-wise increase in the rate as the length of the gap increased. The largest increase in the rate of crosslinking, greater than an order of magnitude, was observed upon changing a nick to a 1-nt gap, thereby introducing five bonds about which to rotate. Subsequent lengthening of the gap afforded smaller increases in the rates. The rate for the 3-nt gap was only twofold slower than the rate with a 17-nt single-stranded overhang (Table 1, ss RNA), suggesting that a 3-nt gap affords nearly the maximal amount of rotational freedom that can be attained.

Crosslinking was also measured with the disulfide at positions ***a*** and ***c***, three and eight base pairs from the 5′ end, respectively. The relative distribution of rates was nearly constant for all three positions tested (Table 1). The absolute rates changed modestly and

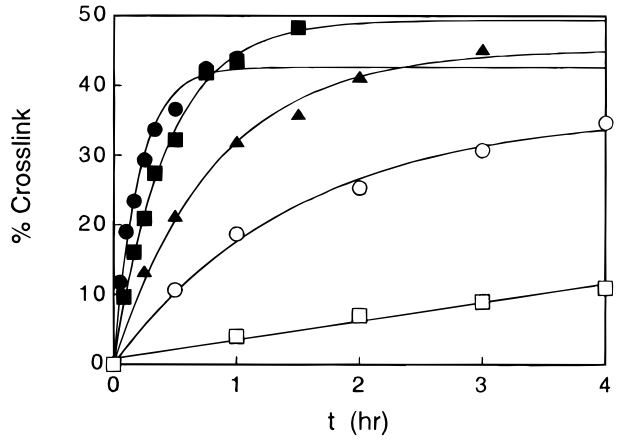

FIGURE 4. Crosslinking as a function of nick or gap length. All reactions contained thiol-modified 30-mer (200 nM), disulfide-modified 13-mer (≤5 nM, modified at position ***b***), sodium chloride (1 M), sodium acetate (50 mM), disodium EDTA (1 mM), Tris buffer (100 mM, pH 7.5, 50 °C), and the appropriate unmodified RNA (300 nM) to yield the corresponding duplex: (●) ss RNA, unmodified RNA not present; (■) 3-nt gap, unmodified 14-mer; (▲) 2-nt gap, unmodified 15-mer; (○) 1-nt gap, unmodified 16-mer; (□) nick, unmodified 17-mer. Each line represents a fit to a single-exponential function (see Materials and Methods).

uniformly between the three positions. These observations suggest that (1) crosslinking is not greatly enhanced by fraying of the end of the RNA duplex near the disulfide, if such fraying occurs at all, and (2) the relative distribution of rates at a given position likely reflects the large-scale motions of the two helical elements rather than a property specific to one position on the duplex.

The data in Table 1 were obtained in 1 M NaCl and with the sequence 5′-UGG-3′ in the gap region. To examine the importance of sequence and ionic conditions, four thiol-modified 30-mers containing A's, C's, G's, or U's in the gap region were prepared and the crosslinking rates measured. A modest two- and threefold difference in rates was observed for the 2-nt and 3-nt gaps, respectively, with U's consistently being the fastest (Tables 2, 3). In both sets of experiments, addition of Mg^{2+} did not yield significant change. The data suggest that the determining factor in the flexibility contributed by a single-stranded gap is having enough bonds about which to rotate, rather than the identity of the base attached to the backbone in the region of rotation.

TABLE 1. First-order rate constants for crosslinking as a function of position and structure.[a]

Structure	Position ***a***	Position ***b***	Position ***c***
ss RNA	0.18 ± 0.04	0.10 ± 0.02	0.075 ± 0.03
3-nt gap	0.085 ± 0.02	0.039 ± 0.01	0.028 ± 0.005
2-nt gap	0.042 ± 0.01	0.021 ± 0.004	0.014 ± 0.003
1-nt gap	0.015 ± 0.003	0.011 ± 0.002	0.0085 ± 0.002
nick	~0.0005	~0.0005	~0.0004

[a]Crosslinking rate constants expressed in units of (min^{-1}). Reactions were conducted at 50 °C in Tris-HCl buffer (100 mM, pH 7.5) with NaCl (1 M), NaOAc (50 mM), EDTA (1 mM), unmodified 14-, 15-, 16-, or 17-mer (300 nM, not present for ss RNA), thiol-modified 30-mer (200 nM), and disulfide-modified 13-mer (≤5 nM).

TABLE 2. First-order rate constants for crosslinking for 2-nt gaps as a function of gap sequence and ionic conditions.[a]

Gap	1000 mM NaCl 0 mM $MgCl_2$	50 mM NaCl 10 mM $MgCl_2$
AA	0.019 ± 0.004	0.021 ± 0.004
CC	0.014 ± 0.003	0.015 ± 0.004
GG	0.022 ± 0.005	0.020 ± 0.004
UU	0.033 ± 0.005	0.026 ± 0.006

[a]Crosslinking rate constants expressed in units of (min^{-1}). Reactions were conducted at 50 °C in Tris-HCl buffer (100 mM, pH 7.5) and contained unmodified 15-mer (300 nM), thiol-modified 30-mer (200 nM), and disulfide-modified 13-mer (≤5 nM, modified at position ***b***).

Comparison of data with previous studies

The results presented here are consistent with qualitative conclusions from an electrophoretic study of DNA containing single-stranded nicks and gaps (Mills et al., 1994). These authors concluded that nicked molecules retain much of their rigid double-helical character, whereas a 1-nt gap results in a large increase in flexibility; gaps of 2–4 nt are more flexible than a 1-nt gap. A distinction in the present work is that crosslinking was observed in the nicked duplex, albeit very slow, suggesting that long-range distortions from a linear conformation are possible in a nicked two-helix junction.

The crosslinking method developed here differs from gel electrophoresis in the interpretation of results. As discussed by Mills et al. (1994), a change in electrophoretic mobility does not distinguish between a stable bend and dynamic bending, whereas crosslinking measures dynamics. Crosslinking would not be observed if a stable bend maintained crosslinking precursors **1** and

TABLE 3. First-order rate constants for crosslinking for 3-nt gaps as a function of sequence and ionic conditions.[a]

Gap	1000 mM NaCl 0 mM $MgCl_2$	50 mM NaCl 10 mM $MgCl_2$
AAA	0.029 ± 0.005	0.027 ± 0.005
CCC	0.024 ± 0.006	0.018 ± 0.004
GGG	0.042 ± 0.008	0.024 ± 0.006
UUU	0.063 ± 0.01	0.038 ± 0.008

[a]Crosslinking rate constants expressed in units of (min^{-1}). Reactions were conducted at 50 °C in Tris-HCl buffer (100 mM, pH 7.5) and contained unmodified 14-mer (300 nM), thiol-modified 30-mer (200 nM), and disulfide-modified 13-mer (≤5 nM, modified at position ***b***).

2 distant from each other; if **1** and **2** were fixed in close proximity, crosslinking would be too fast to measure, as observed previously (Cohen & Cech, 1997). An additional advantage of the crosslinking method is its amenability to changing experimental conditions or protocols, such as working at high ionic strength or studying effects of protein binding.

The small (two- to threefold) difference in crosslinking rates observed for different gap sequences and the effect of base sequence on rate (U > A,G > C; Tables 2, 3) does not correspond to energetic values measured for base-stacking. Turner and co-workers measured the free energy of base-stacking for 3′-dangling ends and found that purines contributed 0.4–1.0 kcal/mol more than did pyrimidines (Freier et al., 1986b). Calculations of base-stacking free energies for ribodinucleoside monophosphates also suggested a preference for the purine–purine interaction (Norberg & Nilsson, 1995). That these trends are not reflected in the data presented in this work suggests that the long-range displacements necessary for crosslinking of duplexes separated by a gap require overcoming an energetic barrier greater than the barrier to disrupt base-stacking.

Implications for natural RNA structures

Our results indicate that two helices separated by only a nick in one strand will retain much of their rigid double-helical character. In contrast, one or more single-stranded nucleotides at a two-helix junction represent points of significant rotational freedom. Thus, natural RNAs containing such two-helix junctions have the potential for undergoing large thermal motions, although tertiary interactions may dampen such motions. For example, the *Tetrahymena* ribozyme contains 3-nt gaps at the P1-P2 and P9-P9.0 junctions, 2-nt gaps at the P2-P2.1 and P7-P3 junctions, and a 1-nt gap at the P3-P8 junction. Despite the overall compact structure of this ribozyme, thermal motions of at least 50 Å occur between P1 and the P3-P8 domain (Cohen & Cech, 1997). To estimate the frequency of these large thermal motions, the second-order rate constant for the thiol–disulfide interchange reaction was used as a scaling factor for the first-order crosslinking rate constants; only a small fraction ($\sim 10^{-9}$) of the encounters result in covalent bond formation (Cohen & Cech, 1997). The observed crosslinking rates in the minutes to hours range correspond to thermal motions on the microsecond time scale, four to six orders of magnitude faster than the rate of chemistry for ribozyme-catalyzed cleavage. The crosslinking rates measured in the model duplexes containing single-stranded gaps are on the order of those measured in the ribozyme. Thus, the long-range bending required for crosslinking in the duplex likely occurs on the micro- to millisecond time scale.

The cleavage site of the hammerhead ribozyme occurs at a two-helix junction (Forster & Symons, 1987). Cleavage of the RNA substrate is favored over ligation of the products, suggesting that cleavage increases the extent of thermal motion in the hammerhead–oligonucleotide complex, thereby making ligation entropically disfavored (Hertel et al., 1994). Our results qualitatively support this interpretation, although tertiary interactions not present in the model duplexes are expected to modulate the frequency, extent, and direction of thermal motions in more complex RNA molecules. Two-helix junctions also occur in the reactants for ligation in the hairpin ribozyme (Hampel et al., 1990) and within P1 of group I introns after the first step of splicing (Cech et al., 1994). Two helices separated by one or more single-stranded nucleotides are found in many other natural RNAs, including RNase P (James et al., 1988) and the snRNAs U2 (Guthrie & Patterson, 1988) and U8 (Sollner-Webb et al., 1993). Some of the aforementioned RNAs exist as ribonucleoprotein complexes and may display dynamic behavior different from that of the free RNA. Comparing the conformational dynamics of free RNAs with their corresponding RNPs represents another application of the thiol–disulfide interchange chemistry to be pursued in future studies.

MATERIALS AND METHODS

General methods

2′-Deoxy-2′-trifluoroacetylamino-5′-dimethoxytrityl-N4-benzoyl cytidine-3′-cyanoethyl phosphoramidite was kindly provided by Dr. Wolfgang Pieken of Nexstar Pharmaceuticals (Boulder, Colorado). A-, C-, G-, and U-ribonucleoside phosphoramidites were obtained from Glen Research. N,N-dimethylformamide, thiophenol, dithiothreitol (DTT), triethylamine, 1-methyl-2-pyrrolidinone, and triethylamine trihydrofluoride were from Aldrich. *N*-succinimidyl-3-(2-pyridyldithio) propionate (**3**) was from Pierce. (γ-^{32}P)-ATP was obtained from New England Nuclear at a specific activity of 6,000 Ci/mmol. A 40% aqueous solution of acrylamide:bisacrylamide (29:1) was obtained from Fisher. T4 polynucleotide kinase (10 units/μL) was from New England Biolabs. TE refers to an aqueous solution of Tris-HCl buffer (10 mM, pH 7.5) and disodium EDTA (1 mM); TEN refers to an aqueous solution of Tris-HCl buffer (10 mM, pH 7.5), disodium EDTA (1 mM), and sodium chloride (250 mM); TBE refers to a buffer composition of Tris base (90 mM), boric acid (90 mM), and disodium EDTA (1 mM). Analytical polyacrylamide gels were affixed on Whatman chromatography paper and quantitated with a Molecular Dynamics 445 SI Phosphorimager.

RNA oligonucleotide preparation

All synthetic RNA oligonucleotides were prepared on an Applied Biosystems 394 RNA synthesizer (1-μmol synthesis scale) using standard phosphoramidite chemistry; deprotection and purification were performed as follows. The solid

support-bound product was suspended in concentrated ammonium hydroxide/ethanol solution [3/1 (v/v), 1.5 mL] and incubated at 55 °C for 8 h in a sealed vial. After cooling to −20 °C, the supernatant was decanted and removed in vacuo. The residue was dissolved in a mixture of triethylamine/1-methyl-2-pyrrolidinone/triethylamine trihydrofluoride [24/46/30 (v/v/v), 400 mL] (Wincott et al., 1995), incubated at 65 °C for 1.5 h, then transferred immediately to TE buffer (5 mL). The resulting solution was desalted over two NAP-25 Sephadex columns (Pharmacia). To the aqueous product solution (7 mL) was added sodium chloride solution (1 M, 1 mL). The product was precipitated by addition of absolute ethanol (24 mL) followed by centrifugation (10,000 × *g*, 2 °C, 30 min). The RNA pellet was dissolved in TE buffer (150 μL) and 80% aqueous formamide solution (150 μL) containing TBE, bromophenol blue (0.05%), and xylene cyanol (0.05%). The oligonucleotide was purified to single-nucleotide resolution by PAGE (20% polyacrylamide and 8 M urea in TBE, gel dimensions $20_h \times 26_w \times 0.3$ cm, 25 W, three oligonucleotide preparations per gel). The product band was visualized by UV shadow and excised. The gel slice was crushed thoroughly and suspended in TEN buffer (10 mL) at 2 °C for 24 h. The supernatant was filtered (0.45-μm cellulose acetate) and the oligonucleotide precipitated by the addition of three volumes absolute ethanol followed by centrifugation (10,000 × *g*, 2 °C, 30 min). The purified RNA oligonucleotide was stored in TE buffer at −20 °C.

Preparation of thiol-modified 30-mers

A 30-mer oligonucletide (20 nmol) containing a unique 2′-amine was dissolved in water (120 μL), sodium borate buffer (1 M, pH 8, 40 μL), and sodium chloride solution (1 M, 20 μL). The solution was warmed to 37 °C and treated with a freshly prepared solution of **3** (500 mM in DMF, 20 μL, 37 °C, 30 min), thus affording the following concentrations: 2′-NH_2 RNA, 100 μM; **3**, 50 mM; sodium borate buffer, 200 mM; NaCl, 100 mM; DMF, 10%. The product was precipitated by addition of absolute ethanol (800 μL) followed by centrifugation (16,000 × *g*, 2 °C, 20 min). The amine modification procedure was repeated once more to afford ≥90% modification. RNA was dissolved in water (140 μL) and sodium borate buffer (1 M, pH 8, 40 μL). The thiol was liberated by treatment with DTT (1 M, 20 μL, 37 °C, 30 min). The reaction was precipitated by addition of absolute ethanol (1 mL) followed by centrifugation (16,000 × *g*, 2 °C, 20 min). To remove remaining DTT, the product was dissolved in TEN buffer (250 μL) and precipitated with absolute ethanol (1 mL). Modified oligonucleotide was stored in TE buffer at −20 °C at a concentration of 20 μM.

Preparation of disulfide-modified 13-mers

The RNA 13-mer (100 pmol) containing a unique 2′-amine was 5′-labeled with γ-^{32}P-ATP (0.5 mCi) and T4 polynucleotide kinase in a volume of 20 μL following standard procedures (Sambrook et al., 1989). The reaction was diluted with water (200 μL) and sodium chloride solution (1 M, 50 μL). RNA was precipitated by addition of absolute ethanol (900 μL) followed by centrifugation (16,000 × *g*, 2 °C, 20 min). Labeled product was dissolved in water (140 μL), sodium borate buffer (1 M, pH 8, 20 μL), and sodium chloride solution (1 M, 20 μL). The solution was warmed to 37 °C and treated with a freshly prepared solution of **3** (500 mM in DMF, 20 μL, 37 °C, 20 min), thus affording the following concentrations: RNA substrate, ~0.5 μM; **3**, 50 mM; sodium borate buffer, 100 mM; NaCl, 100 mM; DMF, 10%. The solution was cooled to 23 °C and treated with thiophenol (70 mM in ethanol, 200 μL, 23 °C, 1 min). The modified RNA was precipitated immediately by addition of absolute ethanol (700 μL) followed by centrifugation (16,000 × *g*, 2 °C, 20 min). The product was dissolved in TE buffer (10 μL) and 80% aqueous formamide solution (10 μL) containing TBE, bromophenol blue (0.05%), and xylene cyanol (0.05%). The RNA was purified to 95% homogeneity by PAGE (20% polyacrylamide and 8 M urea in TBE, gel dimensions $10_w \times 20_h \times 0.05$ cm, 10 W, ~3 h). This provided clean separation from the faster-migrating RNA that remained unmodified after treatment with **3** (~20%). The product band was identified by autoradiography and excised. The gel slice was crushed thoroughly and suspended in TEN buffer (400 μL, 2 °C, 10 min). The product was precipitated by addition of absolute ethanol (2 mL) followed by centrifugation (16,000 × *g*, 2 °C, 20 min). The product was stored in aqueous sodium acetate buffer (10 mM, pH 4.5, 500 μL) at −80 °C in 20-μL aliquots.

Kinetic assay for crosslinking in the three-piece duplex

A stock reaction mixture was prepared by mixing a 40-μL aliquot of water with sodium acetate buffer (1 M, pH 4.5, 30 μL), sodium chloride solution (1 M, 120 μL), disodium–EDTA solution (10 mM, pH 7, 60 μL), thiol-modified 30-mer (1 μM, 120 μL), and a 20-μL aliquot of the disulfide-modified 13-mer (10^5 cpm). Five reaction tubes were prepared, each containing one of the four unmodified RNA strands (1 μM, 30 μL) or water (30 μL). To each of the five tubes was added a 65-μL aliquot of the stock reaction mixture. The solutions were incubated at 70 °C for 1 min followed by 3 min at 50 °C. A 4-μL aliquot was removed and transferred to a 90% aqueous formamide solution (25 μL) containing sodium acetate buffer (100 mM, pH 4.5), bromophenol blue (0.05%), and xylene cyanol (0.05%), then stored frozen on dry ice until gel loading. Crosslinking was initiated at 50 °C by addition of Tris-HCl buffer (1 M, pH 8, 10 μL), thus affording the following concentrations: thiol-modified 30-mer, 200 nM; disulfide modified 13-mer, 5 nM; unmodified RNA, 0 or 300 nM; sodium chloride, 1 M; sodium acetate, 50 mM; disodium EDTA, 1 mM; Tris-HCl buffer, 100 mM (final pH ~7.5). Aliquots of 4 μL were removed over time and transferred to a 90% aqueous formamide solution (25 μL) containing sodium acetate buffer (100 mM, pH 4.5), bromophenol blue (0.05%), and xylene cyanol (0.05%), then stored frozen on dry ice until gel loading. Reaction products were separated by PAGE (20% polyacrylamide and 8 M urea in TBE). Typically, 3–5% crosslinked product was observed during the annealing procedure at pH 4.5; this amount of crosslinking was subtracted from crosslinking occurring after addition of Tris buffer. The resulting data were fit to the equation $y = 1 - [(1 - m)e^{-kt}]$ where y is the fraction crosslinked product, m is the final fraction of crosslink at infinite time, k is the first-order rate constant, and t is time.

ACKNOWLEDGMENTS

We acknowledge Dr. Wolfgang Pieken of Nexstar Pharmaceuticals (Boulder, Colorado) for a generous supply of the 2′-amino-2′-deoxyribose cytidine phosphoramidite. Thanks also to Anne Gooding for oligonucleotide synthesis. T.R.C. is an Investigator and S.B.C. is an Associate of the Howard Hughes Medical Institute.

Received June 15, 1998; returned for revision July 13, 1998; revised manuscript received July 21, 1998

REFERENCES

Benseler F, Williams DM, Eckstein F. 1992. Synthesis of suitably-protected phosphoramidites of 2′-fluoro-2′-deoxyguanosine and 2′-amino-2′-deoxyguanosine for incorporation into oligoribonucleotides. *Nucleosides & Nucleotides 11*:1333–1351.

Cate JH, Gooding AR, Podell E, Zhou K, Golden BL, Kundrot CE, Cech TR, Doudna JA. 1996. Crystal structure of a Group I ribozyme domain: Principles of RNA packing. *Science 273*:1625–1764.

Cech TR, Damberger SH, Gutell RR. 1994. Representation of the secondary and tertiary structure of group I introns. *Nature Struc Biol 1*:273–280.

Cohen SB, Cech TR. 1997. Dynamics of thermal motions within a large catalytic RNA investigated by cross-linking with thiol–disulfide interchange. *J Am Chem Soc 119*:6259–6268.

Forster AC, Symons RH. 1987. Self-cleavage of virusoid RNA is performed by the proposed 55-nucleotide active site. *Cell 50*:9–16.

Freier SM, Kierzek R, Jaeger JA, Sugimoto N, Caruthers MH, Neilson T, Turner DH. 1986a. Improved free-energy parameters for predictions of RNA duplex stability. *Proc Natl Acad Sci USA 83*:9373–9377.

Freier SM, Sugimoto N, Sinclair A, Alkema D, Neilson T, Kierzek R, Caruthers MH, Turner DH. 1986b. Stability of XGCGCp, GCGCYp, and XGCGCYp helixes: An empirical estimate of the energetics of hydrogen bonds in nucleic acids. *Biochemistry 25*:3214–3219.

Guthrie C, Patterson B. 1988. Spliceosomal snRNAs. *Annu Rev Genet 22*:387–419.

Hampel A, Tritz R, Hicks M, Cruz P. 1990. Hairpin catalytic RNA model: Evidence for helices and sequence requirement for substrate RNA. *Nucleic Acids Res 18*:299–304.

Hertel KJ, Herschlag D, Uhlenbeck OC. 1994. A kinetic and thermodynamic framework for the Hammerhead ribozyme reaction. *Biochemistry 33*:3374–3384.

James BD, Olsen FJ, Liu J, Pace NR. 1988. The secondary structure of ribonuclease P RNA, the catalytic element of a ribonucleoprotein enzyme. *Cell 52*:19–26.

Lehnert V, Jaeger L, Michel F, Westhof E. 1996. New loop–loop tertiary interactions in self-splicing introns of subgroup 1C and 1D: A complete 3D model of the *Tetrahymena thermophila* ribozyme. *Chemistry & Biology 3*:993–1009.

Mills JB, Cooper JP, Hagerman PJ. 1994. Electrophoretic evidence that single-stranded regions of one or more nucleotides dramatically increase the flexibility of DNA. *Biochemistry 33*:1797–1803.

Norberg J, Nilsson L. 1995. Stacking free energy profiles for all 16 natural ribodinucleoside monophosphates in aqueous solution. *J Am Chem Soc 117*:10832–10840.

Sambrook J, Fritsch EF, Maniatis T. 1989. *Molecular cloning: A laboratory manual, 2nd ed*. Cold Spring Harbor, New York: Cold Spring Harbor Laboratory Press.

Sigurdsson ST, Tuschl T, Eckstein F. 1995. Probing RNA tertiary structure: Interhelical crosslinking of the hammerhead ribozyme. *RNA 1*:575–583.

Sollner-Webb B, Tyc K, Steitz JA. 1993. Ribosomal RNA processing in eukaryotes. In: Dahlberg AE, Zimmermann RA, eds. *Ribosomal RNA: Structure, evolution, processing, and function in protein synthesis*. Boca Raton, Florida: CRC Press.

Verheyden JPH, Wagner D, Moffatt JG. 1971. Synthesis of some pyrimidine 2′-amino-deoxynucleosides. *J Org Chem 36*:250–254.

Wincott F, DiRenzo A, Shaffer C, Grimm S, Tracz D, Workman C, Sweedler D, Gonzalez C, Scaringe S, Usman N. 1995. Synthesis, deprotection, analysis, and purification of RNA and ribozymes. *Nucleic Acids Res 23*:2677–2684.